applied optics

Design of a brightness-enhancement-film-adaptive freeform lens to enhance overall performance in direct-lit light-emitting diode backlighting

Bin Xie,[1] Run Hu,[1] Qi Chen,[1] Xingjian Yu,[1] Dan Wu,[2] Kai Wang,[3,*] and Xiaobing Luo[1,4]

[1]*School of Energy and Power Engineering, Huazhong University of Science and Technology, Wuhan 430074, China*
[2]*School of Electrical and Electronic Engineering, Nanyang Technological University, Singapore 639798, Singapore*
[3]*Department of Electrical & Electronic Engineering, South University of Science and Technology of China, Shenzhen 518055, China*
[4]*e-mail: luoxb@hust.edu.cn*
Corresponding author: wangk@sustc.edu.cn

In this study, a brightness-enhancement-film- (BEF) adaptive method is proposed to design freeform lenses for enhancing brightness performance in a direct-lit light-emitting diode (LED) backlight system. A detailed design algorithm is presented based on the analysis of the output optical properties of the BEF. By introducing a constriction factor, we can control the light intensity distribution curve at will to adapt to the characteristics of the BEF and make more light transmit through the BEF. Compared with an LED backlight system without a freeform lens, the BEF-adaptive lens method can improve axial luminance by 20.67% and output efficiency by 6.02%.   © 2015 Optical Society of America

OCIS codes: (230.3670) Light-emitting diodes; (220.3630) Lenses; (080.4295) Nonimaging optical systems.

http://dx.doi.org/10.1364/AO.54.005542

1. INTRODUCTION

Light-emitting diodes (LEDs) have been considered as promising light sources with the extraordinary characteristics of high luminous efficiency, low power consumption, long lifetime, and environment protection [1–3]. Currently, LEDs have been widely applied in our daily lives, especially in liquid crystal display (LCD) backlighting.

There are two types of LED backlights, a direct-lit LED backlight and a side-lit LED backlight. A direct-lit LED backlight, compared with a side-lit LED backlight, is not only size scalable but is also able to realize 2D local dimming, which can enhance the contrast ratio and black level of LED TV greatly. Therefore, a direct-lit LED backlight is more commonly used in large-scale LCD displays. A conventional LED direct-lit backlighting unit (BLU) consists of various kinds of elements, for example, light source and optical films. Optical films, such as diffuser planes, diffuser sheets, and brightness enhancement films (BEFs), are used to control the light from light sources for improving luminance, brightness uniformity, color uniformity, and directivity in a conventional BLU.

Among various kinds of optical films, BEFs are the essential element and are widely adopted, which are designed to collimate incident light and improve axial brightness. Since a single prism sheet can only confine light in one direction, BEFs usually consist of two orthogonal prism sheets. As shown in

Fig. 1(a), a typical Vikuiti BEF consists of polyethylene tereph- thalate (PET) substrate with a thickness of 125 μm and an acrylic prism structure with a thickness of 25 μm. Its optical characteristics are shown in Fig. 1(b) [4]. In Fig. 1(b), when Lambertian-distributed light energy is incident upon the inter- face of the prism sheet and air, about 36.8% of the incident light can transmit through the BEF and about 46.3% is re- flected back. Although the light reflected back can be recycled, the efficiency of the BEF is still at a low level (∼50%) [5] and leads to a low output efficiency of the backlight system, which is defined as the percentage of light energy that exits from the backlight system compared to the light energy emitted from LED sources [5–7].

Some solutions have been proposed to improve the output efficiency of backlight systems, such as the optimization of an- gular placements of the LEDs with cone-shaped caps [8], the arrangement of the microstructures by two guiding modes [9], the use of dual-cone-shaped lens caps for improving brightness and uniformity [10]. However, there is little literature referring to the optimization of output light distribution from a light source which adapt to the optical properties of the BEF.

In this study, we propose a BEF-adaptive design method of a freeform lens to improve both output efficiency and axial luminance of the BLU while considering the characteristics of BEFs. The optical designs were validated by Monte Carlo
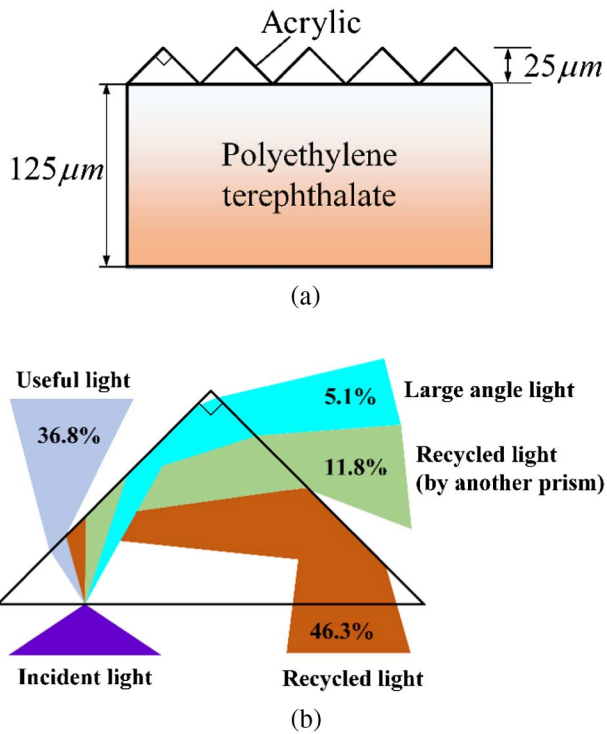
Fig. 1. (a) Structure of a typical 90/50 BEF and (b) its light performance under different incident angles.

ray tracing simulations. Comparisons of luminance performance between the BLU integrated with and without a BEF-adaptive lens were conducted, and the best configuration of the BEF-adaptive lens is presented.

2. DESIGN METHOD

From Fig. 1(b), it can be seen that the incident angle is the key parameter to determine how many rays can be transmitted and how many rays can be reflected. According to the transmittance property of BEF, more rays can be transmitted when they are perpendicular to the prism surface. To design a BEF-adaptive lens, the first step is to find the best incident angle range in which the more the incident rays fall in, the more the rays will be transmitted through the BEF. The second problem is to design a freeform lens that can adapt to the BEF's characteristics and redistribute more rays from an LED light source into the best incident angle range.

The design flowchart is shown in Fig. 2. First, the best incident angle range for high BEF transmittance was investigated. Second, a BEF-adaptive lens was designed to match this incident angle range. Then lighting performance of the BLU on the target plane was conducted by Monte Carlo ray tracing simulations. If the simulation result cannot improve the BEF efficiency and axial luminance simultaneously, we optimize the lens by modifying the constriction factor until both output efficiency and axial luminance were enhanced. It is noted that the criterion used to judge the performance varies with the requirements of the backlight system. When the output efficiency is more heavily demanded than brightness, the output efficiency is the primary criterion, and vice versa.
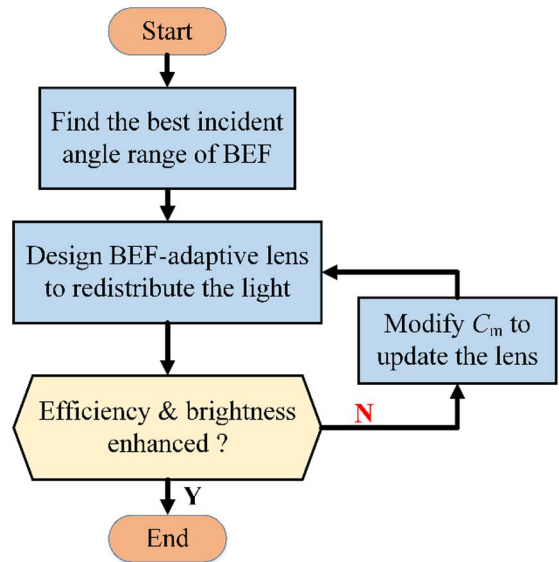

Fig. 2. Flowchart of the design method for a high-luminance LED backlight. C_m is the constriction factor.

Therefore, a specific criterion was determined by a specific design requirement.

A. Finding the Best Incident Angle Range

As shown in Fig. 3, the light source was divided into 18 segments in latitudinal direction with $\theta = 0$–5, 5–10, 10–15, …, 85–90 deg, respectively. Then BEF transmittance of each segmental source was investigated by Monte Carlo ray tracing simulation, which is conducted by optical software LightTools. By doing so, a best incident angle range $\theta = \theta_1 - \theta_2$ was selected to generate the original output light intensity distribution curve (LIDC).

The LIDC can be denoted as the function of the emitting angle θ, $I_{in}(\theta)$, where θ is the angle between the ray and the z-axis. In the same way, the original output LIDC previously mentioned can be expressed as

$$I_{ou\_origin}(\theta) = \begin{cases} 0, & \theta < \theta_1 \;\&\; \theta > \theta_2, \\ I_{in}(\theta), & \theta_1 \le \theta \le \theta_2. \end{cases} \quad \textbf{(1)}$$

B. Redistribution of Original Output LIDC

Now we can redistribute more light into the best incident angle range to improve the output efficiency. However, for the sake
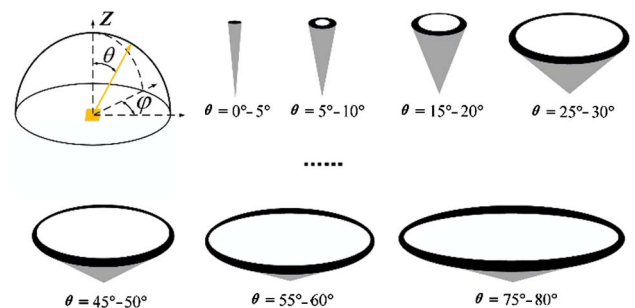

Fig. 3. Segmental light sources within different latitudinal incident angles θ.

of high axial luminance, light energy should be concentrated on a latitudinal angle range which deserves high axial luminance. Therefore, there is a tradeoff between enhancement of output efficiency and axial luminance. (Section 3.B explains the tradeoff operation in detail.) We chose a compromise latitudinal incident angle θ_m to redistribute the original LIDC.

The redistribution process includes two steps: energy division of the original output LIDC and energy readjustment by compressing the original output LIDC. The original output light energy $\Phi_{\mathrm{ou\_origin}}$ could be regarded as composed of N parts of energy unit $\phi_{\mathrm{ou\_origin}}$, according to the algorithm of freeform lens design [11], the luminous flux of each energy unit and total luminous flux of the output energy can be expressed as follows:

$$
\begin{aligned}
\phi_{\mathrm{ou\_origin}} &= \int I_{\mathrm{ou\_origin}}(\theta)\mathrm{d}\omega \\
&= \int_{\varphi_1}^{\varphi_2}\mathrm{d}\varphi \int_{\theta_1}^{\theta_2} I_{\mathrm{ou\_origin}}(\theta)\sin\theta\mathrm{d}\theta,
\end{aligned} \quad \textbf{(2)}
$$

$$
\Phi_{\mathrm{ou\_origin}} = \int_0^{2\pi}\mathrm{d}\varphi \int_0^{\pi/2} I_{\mathrm{ou\_origin}}(\theta)\sin\theta\mathrm{d}\theta, \quad \textbf{(3)}
$$

where φ is the longitudinal azimuth angle and θ is the latitudinal azimuth angle of light energy. Since the total luminous flux of the output energy is divided into N parts, the field angle $\Delta\theta_{\mathrm{ou\_i}}$ of each energy unit along the latitudinal direction can be obtained by iterative calculation as follows:

$$
\begin{aligned}
2\pi\int_{\theta_{\mathrm{ou\_i}}}^{\theta_{\mathrm{ou\_i+1}}} I_{\mathrm{ou\_origin}}(\theta)\sin\theta\mathrm{d}\theta \\
= \frac{\Phi_{\mathrm{ou\_origin}}}{N} \qquad (i = 1, 2...N, \theta_1 = 0),
\end{aligned} \quad \textbf{(4)}
$$

$$
\Delta\theta_{\mathrm{ou\_i}} = \theta_{\mathrm{ou\_i+1}} - \theta_{\mathrm{ou\_i}} \qquad (i = 1, 2, ...N). \quad \textbf{(5)}
$$

Thus, the original output LIDC has been divided into N parts with equal luminous flux, and the boundary of each energy unit has been also calculated as $\Delta\theta_{\mathrm{ou\_i}}$.

Then we conducted the energy division of optimized output LIDC with the same method. In order to redistribute the original output LIDC, a constriction factor C was introduced to compress the original output LIDC into a more compact pattern. The constriction factor C can be expressed as follows:

$$
C_i = C_1 \cdot q_1^{i-1} \qquad (i = 1, 2...m, 0 < q_1 < 1), \quad \textbf{(6)}
$$

$$
C_i = C_m \cdot q_2^{i-m} \qquad (i = m+1, m+2...N, q_2 > 1), \quad \textbf{(7)}
$$

where C consists of two geometric progressions, of which the first one is in descending sequence with a common ratio of q_1, and the second one is in ascending sequence with a common ratio of q_2. After integration with the constriction factor, the output energy division Eqs. (4) and (5) can be expressed as

$$
\begin{aligned}
2\pi\int_{\psi_{\mathrm{ou\_i}}}^{\psi_{\mathrm{ou\_i+1}}} I_{\mathrm{ou\_origin}}(\theta)\sin\psi\mathrm{d}\psi \\
= C_i \cdot \frac{\Phi_{\mathrm{ou\_origin}}}{N} \qquad (i = 1, 2...N),
\end{aligned} \quad \textbf{(8)}
$$

$$
\begin{aligned}
\int_{\psi_{\mathrm{ou\_i}}}^{\psi_{\mathrm{ou\_i+1}}} I_{\mathrm{ou\_origin}}(\psi)\sin\psi\mathrm{d}\psi \\
= C_i \int_{\theta_{\mathrm{ou\_i}}}^{\theta_{\mathrm{ou\_i+1}}} I_{\mathrm{ou\_origin}}(\theta)\sin\theta\mathrm{d}\theta \qquad (i = 1, 2...N),
\end{aligned} \quad \textbf{(9)}
$$

$$
\Delta\psi_{\mathrm{ou\_i}} = \psi_{\mathrm{ou\_i+1}} - \psi_{\mathrm{ou\_i}} \qquad (i = 1, 2, ...N). \quad \textbf{(10)}
$$

In this process, the light energy within the range of $\theta_{\mathrm{ou\_i}}$ to $\theta_{\mathrm{ou\_i+1}}$ is redistributed to the range of $\psi_{\mathrm{ou\_i}}$ to $\psi_{\mathrm{ou\_i+1}}$. Due to the addition of the constriction factor, the output light energy on both sides of latitudinal angle θ_m was converged on θ_m. According to law of energy conservation, the relationship between C_1, q_1, and C_{m+1}, q_2 is

$$
\sum_{i=1}^{m} C_i = C_1 \cdot \frac{1 - q_1^m}{1 - q_1} = m, \quad \textbf{(11)}
$$

$$
\sum_{i=m+1}^{N} C_i = C_{m+1} \cdot \frac{1 - q_2^{(N-m)}}{1 - q_2} = N - m. \quad \textbf{(12)}
$$

To avoid a saltation of luminous intensity around θ_m, C_m and C_{m+1} should be approximately equal, this principle provide us a reference to select and modify the common ratio q_1 and q_2. Once C_m is selected, C_{m+1}, q_1, and q_2 are selected as well. Therefore, we can take C_m as a criterion to measure the compression degree of original output LIDC.

C. Construction of the BEF-Adaptive Lens

To establish the light energy mapping relationship between the light source and the optimized output LIDC, the light source energy was divided into N parts with equal luminous flux as well. The boundary of each energy unit can be expressed as

$$
2\pi\int_{\theta_{\mathrm{in\_i}}}^{\theta_{\mathrm{in\_i+1}}} I_{\mathrm{in}}(\theta)\sin\theta\mathrm{d}\theta = \frac{2\pi}{N}\int_0^{\pi/2} I_{\mathrm{in}}(\theta)\sin\theta\mathrm{d}\theta, \quad \textbf{(13)}
$$

$$
\Delta\theta_{\mathrm{in\_i+1}} = \theta_{\mathrm{in\_i+1}} - \theta_{\mathrm{in\_i}}. \quad \textbf{(14)}
$$

As the mapping relationship between emitting angle of input rays and exiting angle of output rays has been established, the ray mapping method to design a freeform lens to realize this relationship could refer to previous studies [12–17].

3. DESIGN EXAMPLES

We will take the direct-lit LED backlight as an example to validate this design method. The optical components in a typical LED BLU system include a back-reflector, LED light sources, a first diffuser, BEFs, a second diffuser, and a liquid crystal panel. The back-reflector is usually a plane with diffuse reflection or specular reflection, which recycles the reflected light rays. Diffuser sheets are used to ensure uniform spacing and angular distribution of the output light energy [18]. Therefore, here we mainly discuss the optical properties of a typical direct-lit LED backlight system with a back-reflector, LED light sources, and the optical films mentioned above. Then optimize the output LIDC by a BEF-adaptive lens to improve output efficiency and axial luminance simultaneously in the whole radiation angle.

A. Fundamental Setup of the Backlight System

As shown in Fig. 4, an optical model of a conventional direct-lit LED backlight system was established. A backlight cavity is
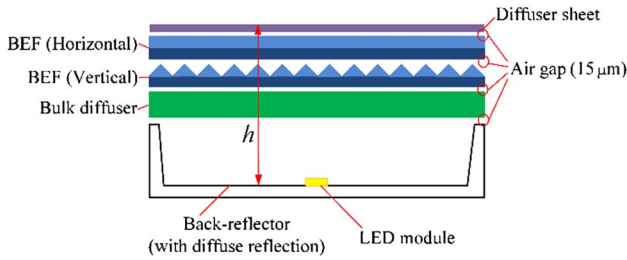
Fig. 4. Optical model of a traditional direct-lit backlight system.

functioned as the back-reflector, by which the internal surface is covered a diffuse reflection material. A typical 3528 SMD LED was used as a light source. Power consumption of this LED module is 0.1 W when driven by 30 mA and its total luminous flux is 9 lm. The size of the LED module is 3.5 mm × 2.8 mm and its LIDC is Lambertian type of $I_{in}(\theta) = I_0 \cos \theta$, where I_0 is the light intensity when the emitting angle $\theta = 0°$. The wavelength of this light source was set as 550 nm [19,20]. In front of the LED light source, there was a bulk diffuser, two orthogonal BEFs, and a diffuser sheet, respectively. A detailed configuration of these optical components is listed in Table 1. Then, a receiving plane with an angular luminance meter was set above the diffuser sheet. The size of the back-reflector is 410 mm × 260 mm and the distance h between the LED light source and the receiver is 18 mm. To simulate the real situation, an air gap of 15 μm was inserted between every two optical stacks.

### B. Design Results and Optical Validation

Then simulation of the BEF output efficiency under a range of different latitudinal angles was conducted and the results are shown in Fig. 5(a). Simulated analysis shows that emitted light with $\theta = 20$–80 deg is efficient to pass through the double-layer BEFs. Then the original output LIDC can be expressed as follows:

$$I_{ou\_origin}(\theta) = \begin{cases} 0, & \theta < 20° \ \& \ \theta > 80°, \\ I_0 \cos \theta, & 20° \le \theta \le 80°. \end{cases} \quad (15)$$

According to Fig. 5, to improve the output efficiency of the backlight module, light energy should be concentrated at $\theta = 60°$. However, for the purpose of improving the axial luminance, light energy should be compressed to an angle range of $\theta = 45°$–50°, which will not cause divarication of the luminance distribution. Therefore, to improve the output efficiency

Table 1. Detailed Configuration of Optical Stacks in the Backlight System

Optical Component	Dimensions (mm)	Optical Properties
Back-reflector	420 × 270 × 19	90% diffuse reflection
Bulk diffuser	420 × 270 × 2	94.5% transmittance, 98.2% haze
BEF	420 × 270 × 0.155	Vikuiti 90/50 BEF [4]
Diffuser sheet	420 × 270 × 0.1	98.9% transmittance, 96.8% haze
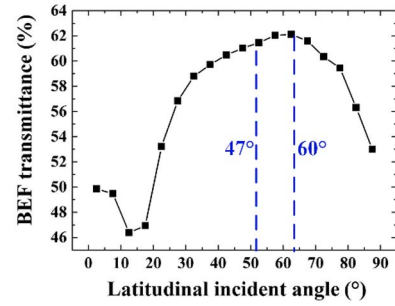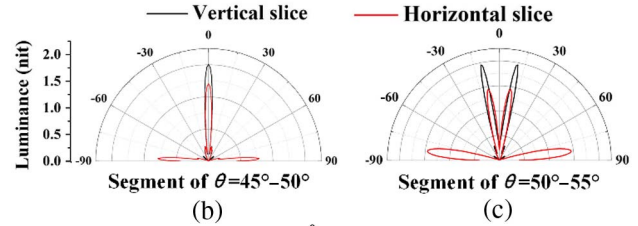
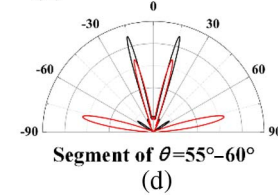**Fig. 5.** (a) Simulated BEF transmittance produced by each latitudinal segmental source; luminance distribution produced by segmental source of (b) $\theta = 45°$–50°, (c) $\theta = 50°$–55°, and (d) $\theta = 55°$–60°.

and axial luminance simultaneously, the compromise incident angle was chosen as $\theta_m = 47°$.

Based on the algorithm of freeform lens design, a series of BEF-adaptive lenses under different constriction factors C_m were designed based on polymethyl methacrylate material, as shown in Fig. 6. The height of the BEF-adaptive lens is 5 mm, and the radius of the inner hemispherical surface is 3 mm. A draft angle of 2.5° on the outer freeform surface was designed, which would ensure a smooth demolding in the injection molding process. Figure 7 shows the LIDC of the BEF-adaptive lens with different C_m. From the curves, it is seen that the decreasing C_m contributes to a heavier compression of LIDC, while the incident angles (corresponding to the peak intensity value) remain at 47°, as designed in Fig. 5.

Then Monte Carlo ray tracing simulations with 5 million rays were conducted, and the peak error estimate (defined as the ratio of the standard deviation of data values with the highest value) is less than 0.8%. In Fig. 8, the results show that axial luminance and output efficiency vary with C_m. For the BLU
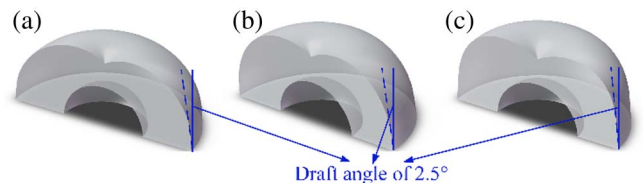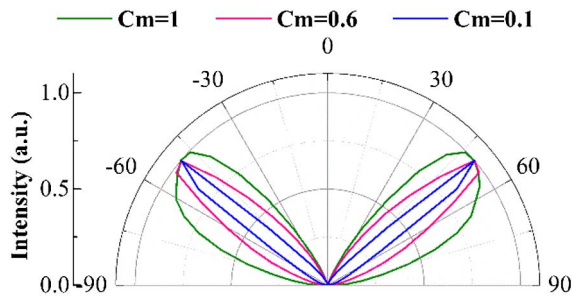

Fig. 6. Models of the BEF-adaptive lens under different constriction factors: (a) $C_m = 1$, (b) $C_m = 0.6$, and (c) $C_m = 0.1$.
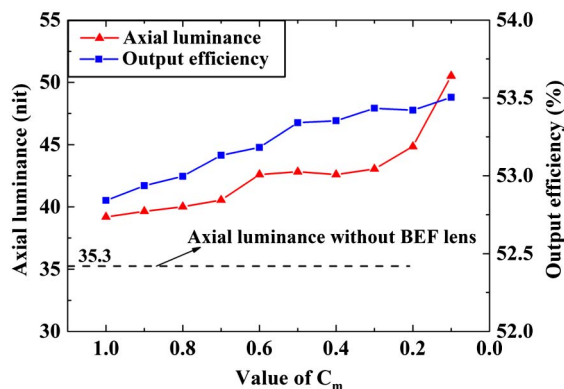
Fig. 7. Light intensity distribution of the BEF-adaptive lens under different constriction factors: $C_m = 1$, $C_m = 0.6$, and $C_m = 0.1$.
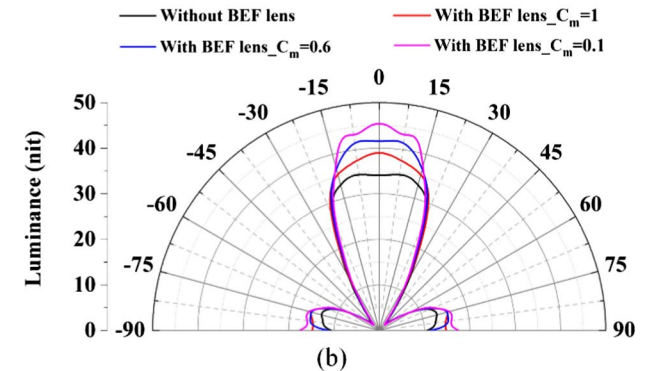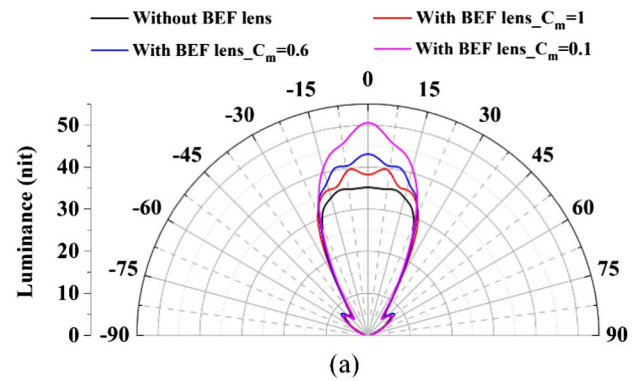
without the BEF-adaptive lens, the output efficiency is 50.16% and axial luminance is 35.3 nit. While for the one with the BEF-adaptive lens of $C_m = 1$, the output efficiency is improved to 52.84%, and the axial luminance is improved to 39.2 nit. Moreover, axial luminance and output efficiency have a similar trend with the variation of C_m, which illustrates that the compression process makes the output light energy more adaptive to BEFs.

For the backlight system, the viewing angle is another critical evaluation parameter [21]. In the simulation, the viewing angles with different C_m were investigated as well and the results are shown in Figs. 9 and 10. Figure 9 shows the horizontal and vertical luminance distribution under different C_m. In Fig. 10, the horizontal axis is the C_m which varies from 1.0 to 0.1, and the left and right vertical axes are the viewing angle and output efficiency, respectively. From the figures we can see that both horizontal and vertical viewing angles decreased with the decrease of C_m. When C_m is below 0.3, the viewing angle decreased sharply.

Taking both axial luminance and viewing angle into account, an optimal C_m of 0.6 was obtained. Under this optimal C_m, the axial luminance and output efficiency increase from 35.3 nit to 42.6 nit and from 50.16% to 53.18%, respectively, while the viewing angle only decreases slightly by 2°. Therefore, coupled with an optimal BEF-adaptive lens, the overall output efficiency and the axial luminance can be enhanced by 6.02% and 20.67%, respectively, without causing a large decrease in the viewing angle.


(a)

(b)

Fig. 9. (a) Horizontal axial luminance distribution and (b) vertical axial luminance distribution under different C_m.

Furthermore, realistic objectives for an LED backlight system are high efficiency, high axial luminance within a specific viewing angle, and high uniformity of spatial luminance [22,23]. Since a comparison of output efficiency, axial luminance, as well as viewing angle between the backlight system with and without a BEF-adaptive lens was illustrated above, it is essential to validate the spatial luminance uniformity of the backlight system integrated with the optimal BEF-adaptive lens.

Based on the direct-lit LED backlight system established above, a typical 3528 LED array with a square dimension distribution was placed in the center of the backlight cavity with


Fig. 8. Output efficiency and axial luminance of the backlight system under different C_m.
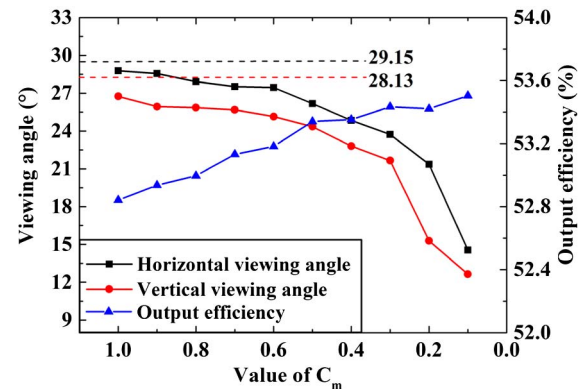
**Fig. 10.** Horizontal viewing angle and vertical viewing angle of the BLU under different C_m.

90% diffuse reflection walls. Considering periodic distribution of the LED modules array, an area with the size of a 6 × 6 LED array was set as the testing area, which is able to reflect the whole lighting performance on the receiving plane, and the horizontal and vertical distance of every two light sources is 18 mm. A spatial luminance meter was set above the receiving plane with the longitude angle and the latitude angle as 0, which indicates that the spatial luminance meter is facing directly toward the backlight module. The distance from the spatial luminance meter to the top of optical stacks is 100 mm, and the half cone angle of the meter is set as 30 deg. In addition, since part of the light emitted by the outside LED modules will be reflected by the backlight cavity, only the luminance uniformity U (defined as the ratio of the minimum luminance value with the average luminance value) of central area of a 4 × 4 LED modules array is considered in this validation.

Then Monte Carlo ray tracing simulations by 7 million rays were performed with a peak error estimate of less than 0.6%, and the spatial luminance distribution of the backlight module

without and with the optimal BEF-adaptive lens were obtained, as shown in Figs. 11(a) and 11(b). For a traditional backlight system without the BEF-adaptive lens, the spatial luminance uniformity is at a high level of 0.87 (5872 nit/6775 nit), when integrated with the optimal BEF-adaptive lens, the spatial luminance uniformity is 0.86 (6031 nit/7049 nit), which indicates that spatial luminance uniformity is approximately constant in these two cases. Therefore, a backlight system with the optimal BEF-adaptive lens can achieve good performance in spatial luminance uniformity. In addition, when excluding the top diffuser sheet, the spatial luminance distributions without/with the optimal BEF-adaptive lens were simulated as well, and the results are shown in Figs. 12(a) and 12(b). Due to the lack of a diffuser sheet, the backlight system without/with a BEF-adaptive lens achieved a spatial luminance uniformity of 0.80 (6382 nit/7958 nit) and 0.79 (6718 nit/8487 nit), respectively. Comparing Fig. 12 with Fig. 11, we see that a top diffuser sheet would decrease the brightness of the whole system but enhance the spatial luminance uniformity.
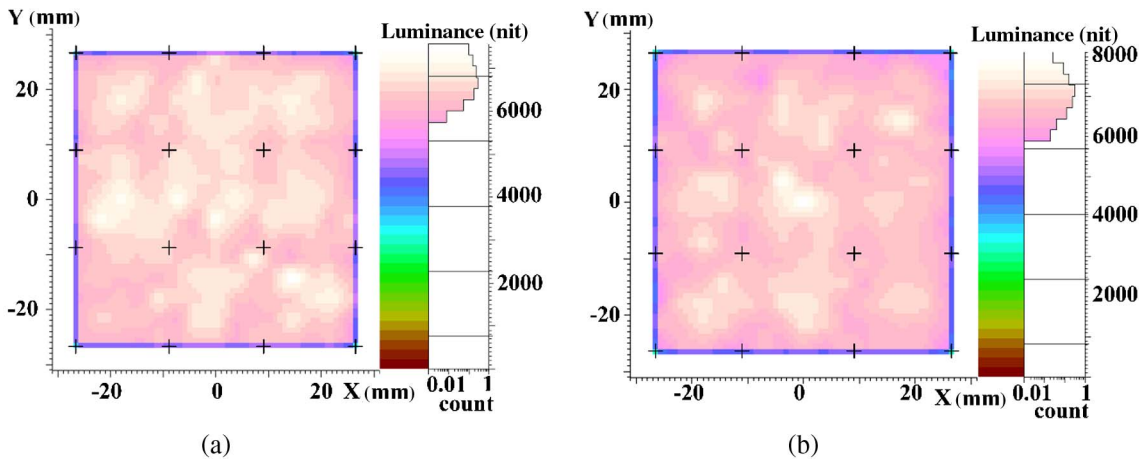
Fig. 11. Spatial luminance distribution of the backlight system (including a diffuser sheet) (a) without and (b) with the BEF-adaptive lenses. (Black crosses indicate the positions of the LED sources.)
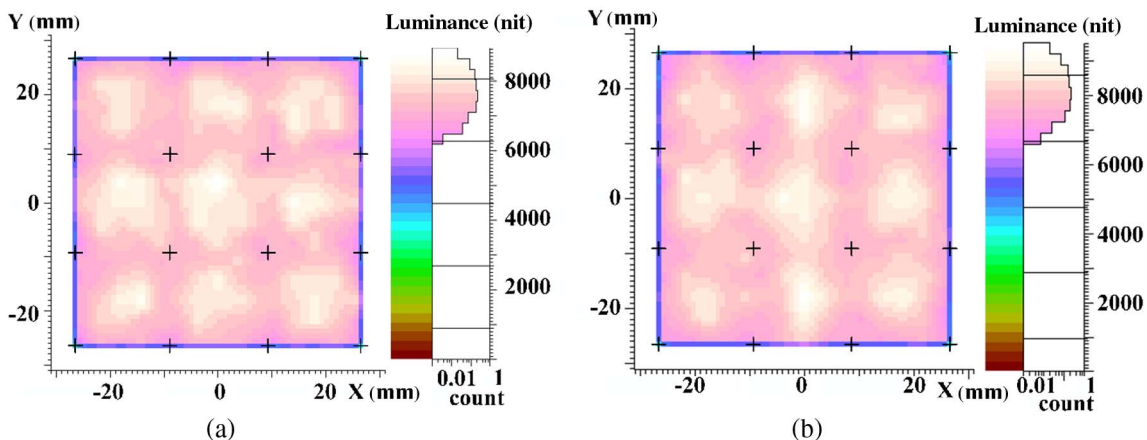
Fig. 12. Spatial luminance distribution of the backlight system (excluding a diffuser sheet) (a) without and (b) with the BEF-adaptive lenses. (Black crosses indicate the positions of LED sources.)

4. CONCLUSIONS

In this study, a BEF-adaptive design method was proposed to achieve high output efficiency and high axial luminance in an LED backlight unit. The main idea is to redistribute the light into the best incident angle range of the BEF to enhance the BEF's output efficiency. A series of freeform lenses with different C_m were designed and Monte Carlo ray tracing simulations were conducted to validate the design. An optimization was done to obtain the best C_m. Under the optimal BEF-adaptive lens of $C_m = 0.6$, the output efficiency increases from 50.16% to 53.18% and axial luminance increases from 35.3 nit to 42.6 nit, while the spatial luminance uniformity is approximately constant at a high level of more than 0.8, and the viewing angle only decreases slightly by 2°. Therefore, this design method provides a flexible design freedom to achieve high axial luminance and overall output efficiency. Since different backlight systems have different requirements for brightness and viewing angle, contributions of the BEF-adaptive lens depends on the specific demand, which means the brightness enhancement by an optimal BEF-adaptive lens is not confined to 20.67%. For a backlight system which requires higher efficiency and brightness, this BEF-adaptive design method is effective to achieve high overall performance with more design freedom.

REFERENCES

1. S. Pimputkar, J. S. Speck, S. P. DenBaars, and S. Nakamura, "Prospects for LED lighting," Nat. Photonics **3**, 180–182 (2009).
2. S. Liu and X. B. Luo, *LED Packaging for Lighting Applications: Design, Manufacturing and Testing* (Wiley, 2011).
3. R. Hu, X. B. Luo, and S. Liu, "Design of a novel freeform lens for LED uniform illumination and conformal phosphor coating," Opt. Express **20**, 727–737 (2012).
4. Vikuiti Brightness Enhancement Film, http://solutions.3m.com/wps/portal/3M/en_US/VikuitiHome.
5. J.-W. Pan and C.-W. Fan, "High luminance hybrid light guide plate for backlight module application," Opt. Express **19**, 20079–20087 (2011).
6. W. Zhang, H. Wang, L. Ji, and C. Liu, "Design and simulation of the LGP structure for LED backlight," Proc. SPIE **7655**, 765537 (2010).
7. AU Optronics Corporation, http://www.auo.com.
8. P. C. P. Chao, C. H. Tsai, J. D. Li, and W. D. Chen, "Optimizing angular placements of the LEDs in a LCD backlight module for maximizing optical efficiency," Microsyst. Technol. **19**, 1669–1678 (2013).
9. C. Y. Li and J. W. Pan, "High-efficiency backlight module with two guiding modes," Appl. Opt. **53**, 1503–1511 (2014).
10. J. G. Chang, L. D. Liao, and C. C. Hwang, "Enhancement of the optical performances for the LED backlight systems with a novel lens-cap," Proc. SPIE **6289**, 62890X (2006).
11. K. Wang, D. Wu, Z. Qin, F. Chen, X. B. Luo, and S. Liu, "New reversing design method for LED uniform illumination," Opt. Express **19**, A830–A840 (2011).
12. F. Chen, S. Liu, K. Wang, Z. Y. Liu, and X. B. Luo, "Free-form lenses for high illuminance quality light-emitting diode MR16 lamps," Opt. Eng. **48**, 123002 (2009).
13. K. Wang, F. Chen, Z. Y. Liu, X. B. Luo, and S. Liu, "Design of compact freeform lens for application specific light-emitting diode packaging," Opt. Express **18**, 413–425 (2010).
14. L. Wang, K. Y. Qian, and Y. Luo, "Discontinuous free-form lens design for prescribed irradiance," Appl. Opt. **46**, 3716–3723 (2007).
15. Y. Luo, Z. Feng, Y. Han, and H. Li, "Design of compact and smooth free-form optical system with uniform illuminance for LED source," Opt. Express **18**, 9055–9063 (2010).
16. D. Ma, Z. Feng, and R. Liang, "Freeform illumination lens design using composite ray mapping," Appl. Opt. **54**, 498–503 (2015).
17. Y. Ding, X. Liu, Z. R. Zheng, and P. F. Gu, "Freeform LED lens for uniform illumination," Opt. Express **16**, 12958–12966 (2008).
18. J. G. Chang and Y. B. Fang, "Dot-pattern design of a light guide in an edge-lit backlight using a regional partition approach," Opt. Eng. **46**, 043002 (2007).
19. Z. Qin, K. Wang, F. Chen, X. Luo, and S. Liu, "Analysis of condition for uniform lighting generated by array of light emitting diodes with large view angle," Opt. Express **18**, 17460–17476 (2010).
20. C.-C. Sun, W.-T. Chien, I. Moreno, C.-T. Hsieh, M.-C. Lin, S.-L. Hsiao, and X.-H. Lee, "Calculating model of light transmission efficiency of diffusers attached to a lighting cavity," Opt. Express **18**, 6137–6148 (2010).
21. C. C. Sun, I. Moreno, S. H. Chung, W. T. Chien, C. T. Hsieh, and T. H. Yang, "Direct LED backlight for large area LCD TVs: brightness analysis," Proc. SPIE **6669**, 666909 (2007).
22. G. T. Boyd, L. R. Whitney, R. A. Miller, and K. M. Kotchick, "Backlighting transmissive displays," U.S. Patent 6663262 (16 December 2003).
23. T.-C. Teng and L.-W. Tseng, "Slim planar apparatus for converting LED light into collimated polarized light uniformly emitted from its top surface," Opt. Express **22**, A1477–A1490 (2014).